



The roles of active site residues in the catalytic mechanism of methylaspartate ammonia-lyase[☆]

Hans Raj, Gerrit J. Poelarends*

Department of Pharmaceutical Biology, Groningen Research Institute of Pharmacy, University of Groningen, Antonius Deusinglaan 1, 9713 AV Groningen, The Netherlands

ARTICLE INFO

Article history:

Received 19 June 2013

Received in revised form 2 July 2013

Accepted 3 July 2013

Keywords:

Methylaspartate ammonia-lyase

Deamination

Enzyme mechanism

Amino acid

Mutagenesis

ABSTRACT

Methylaspartate ammonia-lyase (MAL; EC 4.3.1.2) catalyzes the reversible addition of ammonia to mesaconate to yield L-threo-(2S,3S)-3-methylaspartate and L-erythro-(2S,3R)-3-methylaspartate as products. In the proposed minimal mechanism for MAL of *Clostridium tetanomorphum*, Lys-331 acts as the (S)-specific base catalyst and abstracts the 3S-proton from L-threo-3-methylaspartate, resulting in an enolate anion intermediate. This enolic intermediate is stabilized by coordination to the essential active site Mg²⁺ ion and hydrogen bonding to the Gln-329 residue. Collapse of this intermediate results in the release of ammonia and the formation of mesaconate. His-194 likely acts as the (R)-specific base catalyst and abstracts the 3R-proton from the L-erythro isomer of 3-methylaspartate, yielding the enolic intermediate. In the present study, we have investigated the importance of the residues Gln-73, Phe-170, Gln-172, Tyr-356, Thr-360, Cys-361 and Leu-384 for the catalytic activity of *C. tetanomorphum* MAL. These residues, which are part of the enzyme surface lining the substrate binding pocket, were subjected to site-directed mutagenesis and the mutant enzymes were characterized for their structural integrity, ability to catalyze the amination of mesaconate, and regio- and diastereoselectivity. Based on the observed properties of the mutant enzymes, combined with previous structural studies and protein engineering work, we propose a detailed catalytic mechanism for the MAL-catalyzed reaction, in which the side chains of Gln-73, Gln-172, Tyr-356, Thr-360, and Leu-384 provide favorable interactions with the substrate, which are important for substrate binding and activation. This detailed knowledge of the catalytic mechanism of MAL can serve as a guide for future protein engineering experiments.

© 2013 The Authors. Published by Elsevier B.V. on behalf of Federation of European Biochemical Societies. All rights reserved.

1. Introduction

The enzyme methylaspartate ammonia-lyase (MAL; EC 4.3.1.2) catalyzes the reversible addition of ammonia to mesaconate (**1**) to yield L-threo-(2S,3S)-3-methylaspartate (**2**) and L-erythro-(2S,3R)-3-methylaspartate (**3**) as products (Fig. 1) [1,2]. MAL is used by the bacterium *Clostridium tetanomorphum* H1 as part of a catabolic pathway that converts L-glutamate, via **2**, to yield acetyl-CoA [1–3]. In recent years, MAL has gained a lot of interest because of its potential for application in the asymmetric synthesis of a wide variety of aspartic acid derivatives [4–8]. These non-proteinogenic amino acids are highly valuable as tools for biological research and as chiral building blocks for pharma- and nutraceuticals [9–14].

The structure of MAL from *C. tetanomorphum* (PDB: 1KCZ) and that of the isozyme from *Citrobactor amalonaticus* (PDB: 1KKR) have

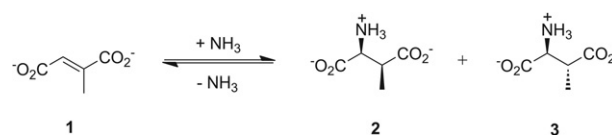


Fig. 1. MAL catalyzed reversible amination of mesaconate (**1**) to yield L-threo-(2S,3S)-3-methylaspartate (**2**) and L-erythro-(2S,3R)-3-methylaspartate (**3**).

been solved by X-ray crystallography [15,16]. On the basis of these structural studies [15–17], combined with kinetic isotope measurements [18,19] and mutagenesis experiments [20], a minimal mechanism has emerged for the MAL-catalyzed reaction. In this proposed mechanism, an (S)-specific (Lys-331) or (R)-specific (His-194) catalytic base abstracts the C3 proton of the respective stereoisomer of 3-methylaspartate to generate an enolate anion intermediate that is stabilized by a hydrogen bond interaction with Gln-329 and coordination to the essential active site Mg²⁺ ion [20]. Collapse of the enolic intermediate results in the elimination of ammonia and yields **1**. This mechanism, however, is far from complete and the importance of other residues for the catalytic activity of MAL has not been investigated yet.

[☆] This is an open-access article distributed under the terms of the Creative Commons Attribution-NonCommercial-No Derivative Works License, which permits non-commercial use, distribution, and reproduction in any medium, provided the original author and source are credited.

* Corresponding author. Tel.: +31 50 3633354; fax: +31 50 3633000.

E-mail address: g.j.poelarends@rug.nl (G.J. Poelarends).

The crystal structure of MAL complexed with its natural substrate **2** shows that the surface of the enzyme lining the substrate binding pocket is provided, in part, by residues Gln-73, Phe-170, Gln-172, Tyr-356, Thr-360, Cys-361 and Leu-384 (Fig. 2) [16]. These residues are highly conserved in known MALs [16], but not in other members of the enolase superfamily [15]. In the present study, we performed site-directed mutagenesis experiments on all these residues to provide insight into their roles in the catalytic mechanism for the MAL-catalyzed reaction. The mutant enzymes were characterized for their structural integrity, ability to catalyze the amination of mesaconate, and regio- and diastereoselectivity. Based on the observed properties of the mutant enzymes, combined with previous structural studies and recent enzyme engineering work, we present a detailed catalytic mechanism for the MAL-catalyzed reaction, with important roles for Gln-73, Gln-172, Tyr-356, Thr-360, and Leu-384 in substrate binding and activation.

2. Materials and methods

2.1. Materials

Mesaconic acid and other chemicals were purchased from Sigma-Aldrich Chemical Co. (St Louis, MO, USA), unless stated otherwise. The sources for the media components, buffers, solvents, pre-packed PD-10 Sephadex G-25 columns, and molecular biology reagents, including PCR purification, gel extraction, and Miniprep kits, are reported elsewhere [20–22]. Oligonucleotides for DNA amplification were synthesized by Operon Biotechnologies (Cologne, Germany).

2.2. Bacterial strains, plasmids and growth conditions

Escherichia coli strain XL1-Blue (Stratagene, La Jolla, CA) was used for cloning and isolation of plasmids. *E. coli* strain TOP10 (Invitrogen) was used in combination with the pBAD/Myc-His A vector (Invitrogen) for recombinant protein production. *E. coli* cells were grown in Luria–Bertani (LB) medium. When required, Difco agar (15 g/L), ampicillin (Ap, 100 µg/mL), and/or arabinose (0.004% w/v) were added to the medium.

2.3. General methods

Techniques for restriction enzyme digestions, ligation, transformation, and other standard molecular biology manipulations were based on methods described elsewhere [23] or as suggested by the manufacturer. PCR was carried out in a DNA thermal cycler (model GS-1) obtained from Biogio (Nijmegen, The Netherlands). DNA sequencing was performed by Macrogen (Seoul, South Korea). Protein was analyzed by polyacrylamide gel electrophoresis (PAGE) under either denaturing conditions using sodium dodecyl sulfate (SDS) or native conditions on gels containing polyacrylamide (10%). The gels were stained with Coomassie brilliant blue. Protein concentrations were determined by the Waddell method [24]. Kinetic data were obtained on a V-650 spectrophotometer from Jasco (IJsselstein, The Netherlands). The kinetic data were fitted by nonlinear regression data analysis by using the Grafit program (Erithacus, Software Ltd., Horley, UK) obtained from Sigma Chemical Co. The CD spectra were recorded on a model 62A-DS spectropolarimeter from AVIV Biomedical Inc. (Lakewood, NJ, USA). ¹H NMR spectra were recorded on a Varian Inova 500 (500 MHz) spectrometer using a pulse sequence for selective presaturation of the water signal. Chemical shifts for protons are reported in parts per million scale (δ scale) downfield from tetramethylsilane and are referenced to protium (H₂O: δ = 4.80).

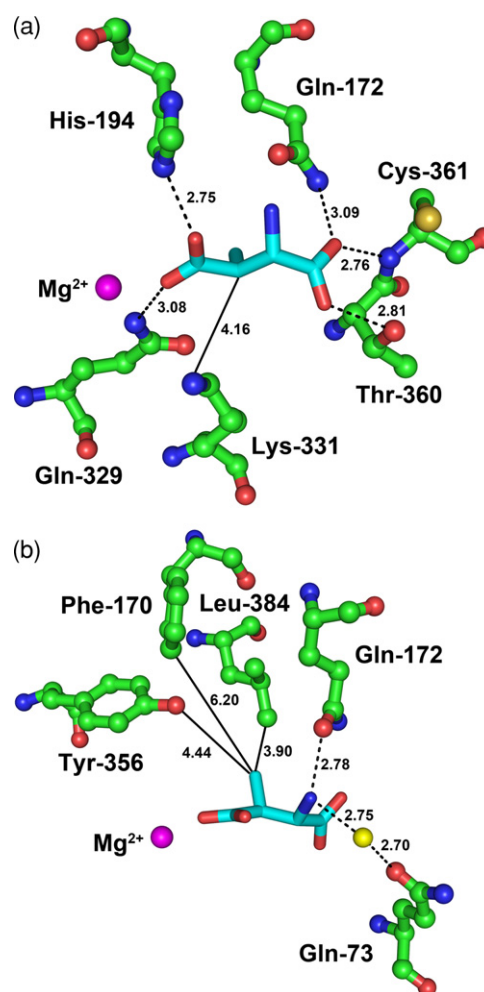


Fig. 2. Crystal structure of MAL in complex with the natural substrate *L*-threo-(2S,3S)-3-methylaspartate (PDB: 1KKR) [16]. (a) Close-up of the active site showing the hydrogen-bond interactions between the substrate's carboxylate groups (C1 and C4) and the side chains of His-194, Gln-329, Gln-172 and Thr-360, or the main chain NH of Cys-361. The carbon atoms of the active site residues are shown in green, and those of the substrate in cyan. Hydrogen bonds are represented as dashed lines. The distance (in Å) between the C3 atom of the substrate and side chain of Lys-331 is shown (atoms connected by a solid line). The magnesium ion is shown as a magenta sphere. (b) Close-up of the active site showing the hydrogen-bond interactions between the substrate's amino group and the side chains of Gln-73 (via a water molecule) and Gln-172, as well as the observed distances (in Å, atoms connected by solid lines) between the substrate's methyl group and the side chains of Leu-384, Phe-170 and Tyr-356. The magnesium ion and water molecule are shown as magenta and yellow spheres, respectively. Colour scheme as in (a). The figures were prepared with Pymol (<http://www.pymol.org>) [30]. (For interpretation of the references to colour in this figure legend, the reader is referred to the web version of this article.)

2.4. Construction, expression and purification of MAL mutants

The MAL mutants were generated by the overlap extension PCR method [25] using plasmid pBAD(MAL-His), which contains the wild-type MAL gene under the transcriptional control of the *araBAD* promoter [20], as the template. The final PCR products were gel-purified, digested with *Nde*I and *Hind*III restriction enzymes, and ligated in frame with both the initiation ATG start codon and the sequence that codes for the polyhistidine region of the expression vector pBADN/Myc-His A. All mutant genes were completely sequenced (with overlapping reads) to verify that only the intended mutation had been introduced. Wild-type MAL and the mutant enzymes were overproduced in *E. coli* TOP10 cells and purified to near homogeneity by following a previously described protocol [20].

2.5. Circular dichroism spectroscopy

Circular dichroism (CD) spectra of the purified wild-type MAL and the purified mutants were measured in Tris–HCl buffer (5 mM, pH 8.0), containing MgCl₂ (2 mM) and KCl (0.1 mM), at a concentration of approximately 3.0 μM in a CD cell with an optical path length of 1.0 mm.

2.6. Kinetic assay

The amination of **1** catalyzed by wild-type or mutant MAL was monitored by following the depletion of **1** at 240 nm or 270 nm in 500 mM Tris–HCl buffer (pH 9.0), containing 20 mM MgCl₂ and 400 mM NH₄Cl, at 30 °C as described previously [20]. The concentration of **1** used in the assay varied in the range 0.1–60 mM.

2.7. Product analysis by ¹H NMR spectroscopy

The amino acid products of the amination of **1** catalyzed by wild-type or mutant MAL were identified by ¹H NMR spectroscopy. Reaction mixtures consisted of 500 μL of a 1 M stock solution of NH₄Cl in water (pH 9.0, containing 20 mM MgCl₂), 100 μL of a 500 mM stock solution of **1** in water (pH 9.0, containing 20 mM MgCl₂), and 100 μL of D₂O. Reactions were started by the addition of 200 μg of freshly purified enzyme, and the reaction mixtures were incubated at 25 °C. ¹H NMR spectra were recorded 2 h and 7 days after the addition of enzyme. Given that MAL catalyzes the fast *anti*-addition and much slower *syn*-addition of ammonia to **1** [20,26,27], leading to *threo*-(2*S*,3*S*)-3-methylaspartate (**2**) and *erythro*-(2*S*,3*R*)-3-methylaspartate (**3**), respectively, we allowed the amination reactions to run for 7 days to detect the formation of low amounts of *erythro* product isomer, if present. Product amounts were estimated by integration of the signals corresponding to **2** and **3** (if present). The ¹H NMR signals for **1**, **2** and **3** have been reported previously [20].

3. Results

3.1. Production, purification and characterization of the MAL mutants

The surface of the protein lining the substrate binding site is provided by the residues shown in Fig. 2 [16]. In a previous study, the roles of residues His-194, Gln-329 and Lys-331 in the catalytic mechanism of the MAL-catalyzed reaction have been investigated by site-directed mutagenesis [20]. The residues selected for mutagenesis in the present study were Gln-73, Phe-170, Gln-172, Tyr-356, Thr-360, Cys-361 and Leu-384 (Fig. 2). Similar to wild-type MAL, all mutant proteins were constructed as His₆-tagged fusion proteins, produced in *E. coli* TOP10 cells, and purified to >95% homogeneity (as assessed by SDS-PAGE) using a one-step Ni-based immobilized metal affinity chromatography procedure [20]. This yielded about 20–30 mg of homogenous protein per liter of cell culture.

Each MAL mutant was analyzed by non-denaturing PAGE (data not shown). The mutant enzymes were found to migrate comparably with the wild-type enzyme, which suggests that the homodimeric association of the mutants was still intact. The structural integrity of each mutant was also assessed by circular dichroism (CD) spectroscopy. The CD spectra of the mutants were comparable to that of wild-type MAL, suggesting that the mutations did not result in any major conformational changes (data not shown).

3.2. Residues that interact with the substrate's 1-carboxylate group

The crystal structure of MAL in complex with **2** shows that the 1-carboxylate group of the substrate has hydrogen-bonding interactions with the main chain NH of Cys-361, the oxygen atom (O_γ) of Thr-360,

Table 1

Apparent kinetic parameters for the amination of mesaconate (**1**) catalyzed by wild-type or mutant MAL.^a

Enzyme	k_{cat} (s ⁻¹)	K_{m} for 1 (mM)	$k_{\text{cat}}/K_{\text{m}}$ (M ⁻¹ s ⁻¹)
MAL ^b	61 ± 1	0.7 ± 0.02	8.7 × 10 ⁴
T360A	0.6 ± 0.1	15 ± 2.5	40
T360S	35 ± 1	1.4 ± 0.3	2.5 × 10 ⁴
C361A	27.5 ± 2.5	2.9 ± 0.5	9.5 × 10 ³
C361K	ND	ND	<0.1
Q172A	>20	>60	3.4 × 10 ²
Q172N	ND	ND	<0.1
Q73A	0.7 ± 0.1	0.2 ± 0.02	3.5 × 10 ³
Q73N	ND	ND	<0.1
F170A	10 ± 1	0.9 ± 0.1	1.1 × 10 ⁴
Y356A	>0.7	>60	12
L384A	>16	>60	2.7 × 10 ²

^a The steady state kinetic parameters were determined in 500 mM Tris–HCl buffer (pH 9.0) containing 20 mM MgCl₂ and 400 mM NH₄Cl at 30 °C. Errors are standard deviations from each fit. ND, not determined.

^b These kinetic parameters were obtained from Raj et al. [20].

and the nitrogen atom (N_{ε2}) of Gln-172 (Fig. 2a) [16]. Residue Gln-172 also interacts, via hydrogen-bonding, with the 2-amino group of the substrate (Fig. 2b) [16]. To investigate the importance of these residues for the catalytic activity and regio- and diastereoselectivity of MAL, six single site-directed mutants were constructed in which Thr-360 was replaced with either an alanine or a serine (T360A and T360S), Cys361 with either an alanine or a lysine (C361A and C361K), and Gln-172 with either an alanine or an asparagine (Q172A and Q172N). The amination activities of the mutants were assayed using **1** as the substrate.

The mutation of Thr-360 to an alanine has a large effect on the catalytic efficiency of MAL. For the T360A mutant, a ~100-fold decrease in k_{cat} and a ~22-fold increase in K_{m} was observed, which results in a ~2200-fold decrease in $k_{\text{cat}}/K_{\text{m}}$ (Table 1). Hence, the major effect of this mutation is on the value of k_{cat} . The mutation of Thr-360 to another residue with an aliphatic hydroxyl group (serine), however, has a less drastic effect on the catalytic efficiency. For the T360S mutant, the $k_{\text{cat}}/K_{\text{m}}$ is reduced only approximately 3.5-fold (Table 1).

Obviously, mutations at position 361 can not eliminate the main chain NH interaction with the substrate. As might therefore be expected, the removal of the side chain at this position, by the substitution of Cys-361 with an alanine, has hardly any effect on the catalytic efficiency of MAL. For the C361A mutant, there is a ~2.2-fold decrease in k_{cat} and an approximately 4.2-fold increase in K_{m} . As a result, the $k_{\text{cat}}/K_{\text{m}}$ is reduced only ~9-fold (Table 1). However, the introduction of a new side chain at position 361, by mutation of Cys-361 to a lysine, essentially abolished enzymatic activity (Table 1). Under the conditions of the kinetic assay, no activity could be detected for this mutant.

The mutation of Gln-172 to an alanine (i.e., removal of the functional side chain) has a large effect on the values of K_{m} and $k_{\text{cat}}/K_{\text{m}}$. For the Q172A mutant, a plot of various concentrations of **1** versus the initial rates measured at each concentration remained linear up to 60 mM. Hence, the Q172A mutant could not be saturated. Accordingly, only the $k_{\text{cat}}/K_{\text{m}}$ was determined, and this parameter is reduced ~255-fold compared to that of wild-type MAL (Table 1). Because the increase in K_{m} for the Q172A mutant is >85-fold, the k_{cat} must be >20 s⁻¹. Surprisingly, the mutation of Gln-172 to an asparagine, which has a side chain with a similar functional group, essentially abolished enzymatic activity (Table 1).

The amination of **1** catalyzed by wild-type MAL and the mutants was also monitored by ¹H NMR spectroscopy to identify the products of the reaction. This spectroscopic analysis showed that the ammonia additions to **1** catalyzed by the MAL mutants lead to the same amino acid product (i.e., 3-methylaspartate) as the corresponding wild-type

Table 2

Conversions and diastereomeric product ratios for the ammonia additions to mesaconate catalyzed by wild-type and mutant MAL.^a

Enzyme	Con. (%) 2 h	d.r. (<i>threo</i> : <i>erythro</i>) ^b	
		after 2 h	after 7 d
MAL	73	89:11	81
T360A	38	93:7	82
T360S	76	86:14	85
C361A	47	>95:5	78
C361K	10	>95:5	70
Q172A	16	>95:5	74
Q172N	6	>95:5	68
Q73A	37	91:9	71
Q73N	18	>95:5	74
F170A	63	>95:5	83
Y356A	24	>95:5	74
L384A	61	>95:5	75

^a Reactions were monitored by ¹H NMR spectroscopy.

^b The d.r. [defined as *threo*-3-methylaspartate (**2**):*erythro*-3-methylaspartate (**3**)] of the amino acid product was determined by comparison of its ¹H NMR signals in the crude reaction mixture to those of authentic standards of **2** and **3**.

MAL-catalyzed reaction. This demonstrates that the mutations at positions 172, 360 and 361 do not affect the regioselectivity of MAL. However, varying diastereomeric product ratios were observed. Consistent with the fact that MAL catalyzes the fast *anti*-addition and the much slower *syn*-addition of ammonia to **1** [20], leading to the *threo* and *erythro* isomers of 3-methylaspartate, respectively, the ¹H NMR spectra recorded after 2 h predominantly showed the formation of **2**, whereas the signals corresponding to **3** mainly appeared in later spectra (Table 2). After 7 days of incubation, the Q172A, T360A, T360S, and C361A mutant-catalyzed amination reactions resulted in 74%, 82%, 85%, and 78% conversion of **1** into the amino acid product with a diastereomeric ratio (d.r.) of 89:11, 54:46, 51:49, and 53:47, respectively (Table 2). The reactions catalyzed by the Q172N and C361K mutants, which have low-level amination activities, resulted in ~70% conversion of **1** into 3-methylaspartate with a d.r. of >95:5 (Table 2).

3.3. Residues that interact with the substrate's 2-amino group

The crystal structure of MAL in complex with **2** shows that the 2-amino group of the substrate has hydrogen-bonding interactions with the oxygen atom (O_{ε1}) of Gln-172 and, via a water molecule, with the nitrogen atom (N_{ε2}) of Gln-73 (Fig. 2b) [16]. The importance of Gln-172 for the catalytic activity of MAL is described above. To investigate the importance of the Gln-73 residue for the catalytic activity and regio- and diastereoselectivity of MAL, this residue was mutated to either an alanine or an asparagine. These mutations are expected to completely remove the functional side chain (Q73A) or to replace the side chain with another one that has a similar functional group (Q73N). The replacement of Gln-73 with an alanine resulted in an active enzyme with a 87-fold reduction in k_{cat} and a 3.5-fold decrease in K_{m} , resulting in a ~25-fold lower $k_{\text{cat}}/K_{\text{m}}$ compared to wild-type MAL (Table 1). Hence, the major effect of this mutation is on the value of k_{cat} . Surprisingly, the Q73N mutant showed very low-level amination activity, preventing the measurement of kinetic parameters (Table 1).

The ammonia additions to **1** catalyzed by the Q73A and Q73N mutants were also monitored by ¹H NMR spectroscopy to identify the amino acid products of these reactions. After a 7 days incubation period, the Q73A- and Q73N-catalyzed amination reactions resulted in 71% and 74% conversion of **1** into 3-methylaspartate with d.r. values of 69:31 and >95:5, respectively (Table 2). No other amino acid products were observed, indicating that the regioselectivity of the enzyme is not influenced by the mutations at position 73.

3.4. Residues lining the binding site for the substrate's 3-methyl group

The crystal structure of MAL in complex with **2** suggests that the side chains of Phe-170, Tyr-356 and Leu-384 are involved in the formation of the binding pocket for the 3-methyl group of the substrate (Fig. 2b) [16]. To study the importance of these residues for the catalytic activity and regio- and diastereoselectivity of MAL, each residue was replaced with an alanine. The mutation of Phe-170 to an alanine resulted in a mutant enzyme with a ~6-fold decrease in k_{cat} and a ~1.3-fold higher K_{m} , which results in an approximately 8-fold decrease in $k_{\text{cat}}/K_{\text{m}}$ (Table 1). The substitutions of Tyr-356 and Leu-384 to an alanine, however, have a larger effect on the catalytic efficiencies of MAL (Table 1). For both the Y356A and L384A mutants, saturation by substrate **1** (up to 60 mM) could not be achieved and therefore only the $k_{\text{cat}}/K_{\text{m}}$ was determined. A 7250- and 320-fold reduction in $k_{\text{cat}}/K_{\text{m}}$ was observed for the Y356A and L384A mutants, respectively. Hence, it is clear that the mutations at positions Tyr-356 and Leu-384 largely influence the K_{m} for **1** (Table 1).

The amination reactions catalyzed by the F170A, Y356A and L384A mutants were also followed by ¹H NMR spectroscopy. After an incubation period of 7 days, the F170A-, Y356A- and L384A-catalyzed reactions resulted in about 83%, 74% and 75% conversion of **1** into 3-methylaspartate with d.r. values of 55:45, 80:20 and 86:14, respectively (Table 2). No other amino acid products were observed, which indicates that the regioselectivity of the enzyme is also not influenced by the mutations at positions 170, 356 and 384.

4. Discussion

On the basis of previous kinetic isotope measurements [18,19], structural studies [15,16], and mutagenesis experiments [20], a minimal mechanism has emerged for the MAL-catalyzed reaction. In this proposed mechanism, Lys-331 acts as the (*S*)-specific base catalyst and abstracts the 3*S*-proton from *L*-*threo*-3-methylaspartate (**2**), resulting in an enolate anion intermediate (**4** in Fig. 3). This enolic intermediate is stabilized by coordination to the essential active site Mg²⁺ ion [28]. Residues His-194 and Gln-329 are thought to assist the Mg²⁺ ion in binding the substrate's 4-carboxylate group and stabilizing the enolate intermediate. Collapse of this intermediate results in the release of ammonia and the formation of mesaconate (**1**). In addition to its proposed role in binding the 4-carboxylate group of the substrate, His-194 is believed to also act as the (*R*)-specific base catalyst and abstracts the 3*R*-proton from the *L*-*erythro* isomer of 3-methylaspartate, yielding the enolic intermediate **4**. The strongest support for this catalytic role of His-194 comes from the observation that the H194A mutant of MAL is highly diastereoselective and can be used as biocatalyst in the synthesis of exclusively the *threo* isomers of various 3-substituted aspartic acids [20,29]. In the present study, guided by the crystal structure of MAL complexed with the natural substrate **2**, we have selected seven other active site residues for site-directed mutagenesis to provide further insight into the catalytic mechanism of MAL. The obtained results allow us to present a full catalytic mechanism for the MAL-catalyzed reaction, detailed knowledge of which can serve as an important guide for future protein engineering experiments.

The crystal structure of MAL in complex with **2** shows that the 1-carboxylate group of the substrate has hydrogen-bond interactions with the main chain NH of Cys-361, O_γ of Thr-360, and N_{ε2} of Gln-172 (Fig. 2a) [16]. To examine the role of Gln-172 and Thr-360 in the mechanism of the MAL-catalyzed reaction, we have mutated these two residues. Complete removal of the functionality at position Thr-360 by replacement with an alanine leads to a ~2200-fold decrease in $k_{\text{cat}}/K_{\text{m}}$ with a ~22-fold increase in the K_{m} for **1**. The same substitution at position Gln-172 also results in a reduced catalytic efficiency with a large increase (>85-fold) in the K_{m} for **1**. These observations, combined with the increase in activity and decrease in K_{m} observed

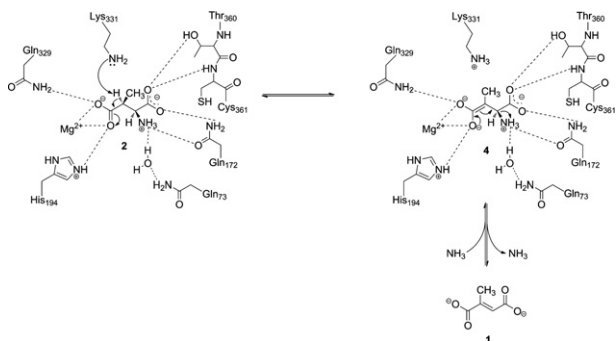


Fig. 3. A schematic representation of the proposed catalytic mechanism of the MAL-catalyzed reaction.

with a serine mutation at position Thr-360, support a role for the side chains of Thr-360 and Gln-172 in assisting the main chain NH of Cys-361 to bind and position the substrate (**1**, **2** or **3**) through hydrogen-bond interactions with its 1-carboxylate group.

The crystal structure of MAL in complex with **2** shows that the 2-amino group of the substrate has hydrogen-bond interactions with O ϵ 1 of Gln-172 and, via a water molecule, with N ϵ 2 of Gln-73 (Fig. 2b) [16]. This suggests roles for the functional groups of these residues in binding the amino group of **2** (or **3**) in the deamination reaction or ammonia in the reverse addition to **1**. Examination of the kinetic properties of the amination reaction catalyzed by the Q73A mutant, which is the only mutation at this position that resulted in an enzyme with significant activity, shows that there is only a minor effect on the value of K_m for **1** (Table 1), suggesting that Gln-73 indeed does not play a role in binding this substrate. One potential explanation for the loss in activity (i.e., reduced k_{cat} value) of the Q73A mutant is that Gln-73 could bind and position ammonia in a favorable orientation for amination of **1**. Support for this view is provided by a recent study in which engineering of the amine binding pocket (i.e., saturation mutagenesis at positions Gln-73 and Gln-172), followed by screening of mutants for enhanced activity towards methylamine addition to **1**, also yielded mutant Q73A [21]. Interestingly, the Q73A mutation moved the specificity of MAL away from ammonia and towards alkylamines. For example, a comparison of k_{cat}/K_m values shows that wild-type MAL is \sim 500-fold more efficient in ammonia addition to **1** than the Q73A mutant, whereas the Q73A mutant is at least 140-fold more efficient in the addition of methylamine to **1**. These observations clearly indicate that Gln-73 is one of the residues that influences the amine specificity of MAL, strongly supporting the proposed role for Gln-73 in binding the amino group of **2** (or **3**) in the deamination reaction or ammonia in the reverse addition to **1**.

The crystal structure of MAL complexed with **2** suggests that the enzyme surface lining the binding site for the 3-methyl group of the substrate is composed almost entirely of side chains, including those of Phe-170, Tyr-356 and Leu-384 (Fig. 2b) [16]. To assess their role in catalysis, we have mutated these residues to an alanine. Examination of the kinetic properties for the Y356A and L384A mutants shows that there is a significant reduction in catalytic efficiency and a large increase ($>$ 85-fold) in the K_m for **1**, suggesting that these residues play a major role in binding the methyl group of the substrate. By contrast to these observations, examination of the kinetic properties for the F170A mutant shows that there is only a small effect of replacing Phe-170 to an alanine on the values of K_m and k_{cat}/K_m , suggesting that Phe-170 is not directly involved in binding the methyl group of the substrate. Consistent with the observed distances between the substrate's methyl group and the side chains of Leu-384, Phe-170 and Tyr-356 (Fig. 2b) [16], our results suggest that additional stabilization of the substrate in the active site is provided by favorable van der Waals packing interactions between the substrate's methyl group and

the side chains of Tyr-356 and Leu-384, while the side chain of Phe-170 is likely too far away to provide a stabilizing interaction. Strong support for the interaction between Leu-384 and the methyl group of the substrate also comes from a recent protein engineering study, in which position Leu-384 was randomized, followed by screening of mutants for amination activity towards 2-hexylfumarate [21]. This approach yielded mutants L384G and L384A, and both mutations moved the specificity of MAL away from mesaconate and towards the unnatural substrate 2-hexylfumarate. Intriguingly, the L384A mutant was shown to exhibit a broad substrate scope, including fumarate derivatives with alkyl, aryl, alkoxy, aryloxy, alkylthio and arylthio substituents at the C2 position. These observations indicate that Leu-384 is one of the residues that influences the substrate (i.e., fumarate) specificity of MAL, supporting a role for Leu-384 in assisting Tyr-356 to bind and position the substrate through van der Waals interactions with its methyl group.

Notably, all mutants described in this study retained the high regioselectivity of the wild-type enzyme, producing 3-methylaspartate as single amino acid product in the amination reaction. Hence, altering the regioselectivity of MAL probably requires the synergistic effects encountered by multiple simultaneous mutations. However, although all mutants exclusively produce 3-methylaspartate, varying diastereomeric ratios (i.e., mixtures of *L-threo* and *L-erythro* isomers of 3-methylaspartate) were observed. Whereas the amination reactions catalyzed by most mutants provided a mixture of *threo* and *erythro* isomers, the amination reactions catalyzed by the C361K, Q172N, and Q73N mutants provided a single diastereoisomer having the *threo* configuration (Table 2). It is important to emphasize that the latter mutants have very low-level amination activities. Given that for wild-type MAL the rate of *anti*-addition is approximately 100-fold higher than the rate for *syn*-addition [20,22,26,27], and assuming that for these mutants both rates are equally reduced by the mutation, the amount of *syn*-addition product (i.e., the *erythro* isomer) formed in the reaction mixture might be too low to detect by ^1H NMR spectroscopy. Hence, these mutant enzymes do not necessarily have altered diastereoselectivities.

On the basis of the results described in this study, the previously proposed minimal mechanism for the MAL-catalyzed deamination reaction can now be extended (Fig. 3). As described above, residues Lys-331, His-194 and Gln-329 and the Mg^{2+} ion play important roles in formation and stabilization of the enolate anion intermediate **4**. In the next step, this enolic intermediate collapses and eliminates ammonia to form the mesaconate (**1**) product. Residues Gln-73 (via a water molecule) and Gln-172 could position and 'lock' the amino group in a favorable orientation for deamination, whereas Thr-360 and Cys-361, assisted by Gln-172, play important roles in binding the substrate's 1-carboxylate group. In addition, residues Tyr-356 and Leu-384 provide stabilizing interactions with the substrate's 3-methyl group. Together, these interactions are important for the optimal positioning and activation of the substrate, and are important determinants of the substrate specificity of MAL. This detailed understanding of the catalytic mechanism of MAL can serve as an important guide for future engineering experiments that aim to further expand the substrate scope of this fascinating enzyme.

Acknowledgements

We gratefully acknowledge Gea K. Schuurman-Wolters (Department of Biochemistry, University of Groningen) for her assistance in acquiring the CD spectra. We thank Pieter van der Meulen (Molecular Dynamics group, University of Groningen) for his assistance in acquiring the NMR spectra. We thank Dr. Wiktor Szymanski (Center for Systems Chemistry, Stratingh Institute of Chemistry, University of Groningen), Dr. Jandre de Villiers (Department of Pharmaceutical Biology, University of Groningen) and Dr. Vinod Puthan Veetil (Department of Pharmaceutical Biology, University of Groningen) for

their insightful discussions. This research was financially supported by a VENI (700.54.401) grant (to G.J.P.) from the Division of Chemical Sciences of the Netherlands Organisation of Scientific Research (NWO-CW).

References

- [1] Barker, H.A., Smyth, R.D., Wilson, R.M. and Weissbach, H. (1959) The purification and properties of β -methylaspartase. *J. Biol. Chem.* 234, 320–328.
- [2] Goda, S.K., Minton, N.P., Botting, N.P. and Gani, D. (1992) Cloning, sequencing, and expression in *Escherichia coli* of the *Clostridium tetanomorphum* gene encoding β -methylaspartase and characterization of the recombinant protein. *Biochemistry* 31, 10747–10756.
- [3] Kato, Y. and Asano, Y. (1997) 3-Methylaspartate ammonia-lyase as a marker enzyme of the mesaconate pathway for (S)-glutamate fermentation in Enterobacteriaceae. *Arch. Microbiol.* 168, 457–463.
- [4] Akhtar, M., Botting, N.P., Cohen, M.A. and Gani, D. (1987) Enantiospecific synthesis of 3-substituted aspartic acids via enzymic amination of substituted fumaric acids. *Tetrahedron* 43, 5899–5908.
- [5] Botting, N.P., Akhtar, M., Cohen, M.A. and Gani, D. (1988) Substrate specificity of the 3-methylaspartate ammonia-lyase reaction: observation of differential relative reaction rates for substrate–product pairs. *Biochemistry* 27, 2953–2955.
- [6] Gulzar, M.S., Akhtar, M. and Gani, D. (1997) Preparation of *N*-substituted aspartic acids via enantiospecific conjugate addition of *N*-nucleophiles to fumaric acids using methylaspartase: synthetic utility and mechanistic implications. *J. Chem. Soc. Perkin Trans. 1*, 649–656.
- [7] de Villiers, M., Puthan Veetil, V., Raj, H., de Villiers, J. and Poelarends, G.J. (2012) Catalytic mechanisms and biocatalytic applications of aspartate and methylaspartate ammonia lyases. *ACS Chem. Biol.* 7, 1618–1628.
- [8] Heberling, M.M., Wu, B., Bartsch, S. and Janssen, D.B. (2013) Priming ammonia lyases and aminomutases for industrial and therapeutic applications. *Curr. Opin. Chem. Biol.* 17, 250–260.
- [9] Shimamoto, K., Sakai, R., Takaoka, K., Yumoto, N., Nakajima, T., Amara, S.G. et al. (2004) Characterization of novel *L*-threo- β -benzyloxyaspartate derivatives, potent blockers of the glutamate transporters. *Mol. Pharmacol.* 65, 1008–1015.
- [10] Shimamoto, K. (2008) Glutamate transporter blockers for elucidation of the function of excitatory neurotransmission systems. *Chem. Rec.* 8, 182–199.
- [11] Mavencamp, T.L., Rhoderick, J.F., Bridges, R.J. and Esslinger, C.S. (2008) Synthesis and preliminary pharmacological evaluation of novel derivatives of *L*- β -threo-benzylaspartate as inhibitors of the neuronal glutamate transporter EAAT3. *Bioorg. Med. Chem.* 16, 7740–7748.
- [12] Kahn, M. (1993) Peptide secondary structure mimetics: Recent advances and future challenges. *Synlett* 11, 821–826.
- [13] Burger, K. and Spengler, J. (2000) A new approach to *N*-methylaspartic, *N*-methylglutamic, and *N*-methyl- α -aminoadipic acid derivatives. *Eur. J. Org. Chem.* 31, 199–204.
- [14] Nofre C., Tinti J.-M. (1996) *N*-substituted derivatives of aspartame useful as sweetening agents. United States Patent No. 5480668.
- [15] Asuncion, M., Blankenfeldt, W., Barlow, J.N., Gani, D. and Naismith, J.H. (2002) The structure of 3-methylaspartase from *Clostridium tetanomorphum* functions via the common enolase chemical step. *J. Biol. Chem.* 277, 8306–8311.
- [16] Levy, C.W., Buckley, P.A., Sedelnikova, S., Kato, Y., Asano, Y., Rice, D.W. et al. (2002) Insights into enzyme evolution revealed by the structure of methylaspartate ammonia lyase. *Structure* 10, 105–113.
- [17] Babbitt, P.C., Hasson, M.S., Wedekind, J.E., Palmer, D.R., Barrett, W.C., Reed, G.H. et al. (1996) The enolase superfamily: a general strategy for enzyme-catalyzed abstraction of the α -protons of carboxylic acids. *Biochemistry* 35, 16489–16501.
- [18] Bright, H.J., Ingraham, L.L. and Lundin, R.E. (1964) The mechanism of the methylaspartate ammonia-lyase reaction: deuterium exchange. *Biochim. Biophys. Acta* 81, 576–584.
- [19] Bright, H. (1964) The mechanism of the β -methylaspartase reaction. *J. Biol. Chem.* 239, 2307–2315.
- [20] Raj, H., Weiner, B., Puthan Veetil, V., Reis, C.R., Quax, W.J., Janssen, D.B. et al. (2009) Alteration of the diastereoselectivity of 3-methylaspartate ammonia lyase by using structure-based mutagenesis. *ChemBioChem* 10, 2236–2245.
- [21] Raj, H., Szymański, W., de Villiers, J., Rozeboom, H.J., Puthan Veetil, V., Reis, C.R. et al. (2012) Engineering methylaspartate ammonia lyase for the asymmetric synthesis of unnatural amino acids. *Nat. Chem.* 4, 478–484.
- [22] Raj, H., Puthan Veetil, V., Szymański, W., Dekker, F.J., Quax, W.J., Feringa, B.L. et al. (2011) Characterization of a thermostable methylaspartate ammonia lyase from *Carboxydotherrmus hydrogenoformans*. *Appl. Microbiol. Biotechnol.* 94, 385–397.
- [23] Sambrook, J., Fritsch, E.F. and Maniatis, T. (1989) *Molecular Cloning: A Laboratory Manual*. 2nd ed. Cold Spring Harbor, NY: Cold Spring Harbor Laboratory Press.
- [24] Waddell, W.J. (1956) A simple ultraviolet spectrophotometric method for the determination of protein. *J. Lab. Clin. Med.* 48, 311–314.
- [25] Ho, S.N., Hunt, H.D., Horton, R.M., Pullen, J.K. and Pease, L.R. (1989) Site-directed mutagenesis by overlap extension using the polymerase chain reaction. *Gene* 77, 51–59.
- [26] Archer, C.H., Thomas, N.R. and Gani, D. (1993) Syntheses of (2*S*,3*R*)-3-methylaspartic and (2*S*,3*R*)-[3-²H]-3-methylaspartic acids – slow substrates for a *syn*-elimination reaction catalyzed by methylaspartase. *Tetrahedron: Asymmetry* 4, 1141–1152.
- [27] Archer, C.H. and Gani, D. (1993) Kinetics and mechanism of *syn*-elimination of ammonia from (2*S*,3*R*)-3-methylaspartic acid by methylaspartase. *J. Chem. Soc. Chem. Commun.* 2, 140–142.
- [28] Bright, H.J. (1967) Divalent metal activation of β -methylaspartase. The importance of ionic radius. *Biochemistry* 6, 1191–1203.
- [29] Raj, H., Szymański, W., de Villiers, J., Puthan-Veetil, V., Quax, W.J., Shimamoto, K., Janssen, D.B., Feringa, B.L. & Poelarends, G.J. (2013) Kinetic resolution and stereoselective synthesis of 3-substituted aspartic acids by using engineered methylaspartate ammonia lyases. *Chem. Eur. J.*, in press (DOI:10.1002/chem.201301832).
- [30] DeLano, W.L. (2002) The PyMOL molecular graphics system. San Carlos, CA, USA: DeLano Scientific (<http://www.pymol.org>).